Stationary Expansion Shocks for a Regularized Boussinesq System

By Gennady A. El, Mark A. Hoefer, and Michael Shearer

Stationary expansion shocks have been identified recently as a new type of solution to hyperbolic conservation laws regularized by nonlocal dispersive terms that naturally arise in shallow-water theory. These expansion shocks were studied previously for the Benjamin-Bona-Mahony (BBM) equation using matched asymptotic expansions. In this paper, we extend the BBM analysis to the regularized Boussinesq system by using Riemann invariants of the underlying dispersionless shallow-water equations. The extension for a system is nontrivial, requiring a combination of small amplitude, long-wave expansions with high order matched asymptotics. The constructed asymptotic solution is shown to be in excellent agreement with accurate numerical simulations of the Boussinesq system for a range of appropriately smoothed Riemann data.

1. Introduction

We consider the normalized form of the classical regularized Boussinesq system for shallow-water waves with dispersion (see, e.g., [1,2])

$$h_t + (uh)_x = 0, \qquad u_t + uu_x + h_x - \tfrac{1}{3}u_{xxt} = 0. \tag{1}$$

The nondimensional variables h, u represent the height of the water free surface above a flat horizontal bottom, and the depth-averaged horizontal component of the water velocity, respectively. System (1) is nonevolutionary,

Address for correspondence: M.A. Hoefer, Department of Applied Mathematics, University of Colorado, Boulder, CO 80309, USA; e-mail: hoefer@colorado.edu

DOI: 10.1111/sapm.12191

STUDIES IN APPLIED MATHEMATICS 00:1–22
© 2017 Wiley Periodicals, Inc., A Wiley Company

that is, not explicitly resolvable with respect to the time derivatives, a property that enables the possibility of new classes of solutions not generally observed in hyperbolic conservation laws and their evolutionary dispersive regularizations such as the Korteweg–de Vries equation, the defocusing nonlinear Schrödinger equation, and other equations exhibiting rich families of dispersive shock waves [3, 4]. New solutions in the form of stationary, smooth, nonoscillatory expansion shocks were found in [5] for the Benjamin-Bona-Mahony (BBM) equation, that represents a unidirectional analog of the system (1).

The Boussinesq equations (1) are a convenient mathematical model in which to study expansion shocks for a system of dispersive equations. More broadly, the Boussinesq equations fall within the class of hyperbolic equations modified to incorporate dispersive terms, rather than dissipative terms, commonly referred to as dispersive hydrodynamic equations [4]. More familiar dispersive hydrodynamic solutions include oscillatory, compressive dispersive shock waves and expansive rarefaction waves. The expansion shock waves described in this work, on the other hand, are monotone, realized as the rapid transition between two noncentered rarefaction waves. Expansion shocks also differ from other dispersive hydrodynamic solutions resulting from certain critical effects such as a loss of convexity in the hydrodynamic flux or linear dispersion. These include kinks, smooth monotone solutions associated with a nonconvex flux or loss of genuine nonlinearity in the case of systems of dispersive equations [5], and resonant, oscillatory dispersive shock waves when the linear dispersion exhibits an inflection point [6].

The physical relevance of expansion shocks is an open question at this time. Within the context of water wave theory, the solutions we construct here are not expected to be physical. The regularized Boussinesq equations (1) are a reduced variant of a class of weakly nonlinear, long wave models of surface water waves [3]. Expansion shocks can be viewed as an example of unintended, artificial phenomena that may be introduced when applying asymptotically equivalent versions of shallow-water equations outside their domain of asymptotic validity. Indeed, it is the nonlocal character of short-wave dispersion in the BBM equation and this version of the Boussinesq equations that is the principal mechanism for the existence of expansion shock solutions.

A stationary shock solution of (1),

$$h(x,t) = \begin{cases} h_-, & x < 0 \\ h_+, & x > 0, \end{cases} \qquad u(x,t) = \begin{cases} u_-, & x < 0 \\ u_+, & x > 0, \end{cases} \tag{2}$$

must satisfy Rankine-Hugoniot (RH) jump conditions

$$h_+ u_+ = h_- u_-; \quad h_+ + \tfrac{1}{2}u_+^2 = h_- + \tfrac{1}{2}u_-^2. \tag{3}$$

Equations (3) can be reformulated to express $u_\pm$ in terms of $h_\pm$ yielding expressions that we refer to as the *RH locus*

$$u_\pm = h_\mp \left(\frac{2}{h_- + h_+} \right)^{1/2}. \tag{4}$$

Note that (2) and (3) are weak solutions of both the hyperbolic system of dispersionless shallow-water equations and the dispersive system (1), due to the shock being time independent. The shock is expansive (in the sense specified below) if and only if $h_+ < h_-$. Expansion shocks do not satisfy Lax entropy conditions [7] and are known to be unstable, immediately giving way to continuous self-similar rarefaction waves in hyperbolic theory. However, for certain types of dispersive regularization, a smoothed stationary expansion shock can persist, exhibiting only slow, algebraic decay with time. This new type of shock wave was identified in the BBM equation [1] by constructing an asymptotic solution of an initial value problem with smoothed jump (Riemann) initial data.

In [5], we also showed numerical simulations of the Boussinesq system (1) with initial conditions for h, u representing smoothed Riemann data with $h_+ < h_-$ satisfying the RH conditions (3) in the far field. The graphs of the variables $h(x,t), u(x,t)$ as time t evolves resemble the structures observed for the evolution of the asymptotic solution of the BBM equation [1]. However, the arguments of that paper do not apply directly to the evolution of stationary shocks for the system (1), and the purpose of this paper is to show how the BBM analysis can be extended to describe Boussinesq expansion shocks. It turns out that the generalization of the analysis of [5] to a system requires some subtle manipulations, including expansions with two parameters and a higher order matched asymptotic analysis. The analysis reveals features of the solution not present in the scalar case. The central idea is to use Riemann invariants of the underlying dispersionless shallow-water system as new field variables in the full dispersive equations (1). Broadly speaking, the Riemann invariant associated with the faster characteristic speed is constant to a high order, while the Riemann invariant of the slower characteristic speed evolves according to the BBM equation. However, a consistent characterization of this broad behavior requires a careful use of matched asymptotic expansions, with precise control of spatial and temporal scaling, in comparison with the initial jump in the data. In the final section, we present results of numerical simulations that are in excellent agreement with the asymptotics, over a surprisingly wide range of parameters. Numerical errors are shown to be consistent with the asymptotic predictions, small inaccuracies being largely explained through higher order terms and wave properties.

2. Expansion shock Riemann data

The shallow-water equations

$$h_t + (uh)_x = 0, \qquad u_t + uu_x + h_x = 0, \tag{5}$$

coincide with the dispersionless limit of the Boussinesq equations (1). System (5) is a hyperbolic system of conservation laws, with flux function $F(h,u) = (uh, \frac{1}{2}u^2 + h)$. We assume that $u > 0$. The characteristic speeds $u \pm \sqrt{h}$ are real and distinct eigenvalues of the Jacobian matrix $dF(h,u)$, for $h > 0$. Because we are assuming $u > 0$, we have $\lambda_2 = u + \sqrt{h} > 0$, whereas $\lambda_1 = u - \sqrt{h}$ can have either sign. The corresponding Riemann invariants

$$s = u + 2\sqrt{h}, \qquad r = u - 2\sqrt{h} \tag{6}$$

diagonalize the system (5), which for smooth solutions becomes

$$s_t + \tfrac{1}{4}(r + 3s)s_x = 0, \qquad r_t + \tfrac{1}{4}(3r + s)r_x = 0. \tag{7}$$

Inverse formulae for h and u in terms of the Riemann invariants are

$$h = \tfrac{1}{16}(s - r)^2, \qquad u = \tfrac{1}{2}(s + r). \tag{8}$$

Rarefaction waves for system (5) are solutions $h(x,t), u(x,t)$, throughout which one of the Riemann invariants is constant. We will consider only rarefaction waves associated with the slow $\lambda_1 = \frac{1}{4}(3r + s)$ characteristic family; s is constant throughout such a wave, but r is constant only on each individual λ_1 characteristic.

As we have mentioned, the stationary shock (2) is a weak solution of both the Boussinesq system (1) and of the shallow-water equations (5). The Lax entropy condition specifies that at each $t > 0$, three of the four characteristics (two for $x > 0$ and two for $x < 0$) should enter the shock, and the fourth should leave. Because $\lambda_2 > 0$, this is equivalent to requiring $\lambda_1(h_-, u_-) > 0$ and $\lambda_1(h_+, u_+) < 0$. If these inequalities are satisfied, we say the shock is *compressive*. If they are reversed, the shock is *expansive.*

We now observe that the stationary shock (2) is compressive if and only if $h_+ > h_-$. Correspondingly, it is expansive if and only if $h_+ < h_-$. To see this, we use (4) to deduce that $\lambda_1(h_-, u_-) = u_- - \sqrt{h_-} = h_+(\frac{2}{h_- + h_+})^{1/2} - \sqrt{h_-} < 0$ if and only if $h_+ < h_-$, and similarly, $\lambda_1(h_+, u_+) = u_+ - \sqrt{h_+} = h_-(\frac{2}{h_- + h_+})^{1/2} - \sqrt{h_+} > 0$ if and only if $h_+ < h_-$.

We note that the scaling

$$\tilde{h} = \frac{h}{H}, \qquad \tilde{u} = \frac{u}{\sqrt{H}}, \qquad \tilde{t} = \sqrt{H}t, \qquad \tilde{x} = x, \tag{9}$$

leaves Equation (1) invariant. Therefore, without loss of generality, we can consider

$$h_+ = 1, \qquad h_- = H. \tag{10}$$

Utilizing the normalization (10) and the RH locus (4), the expansion shock Riemann data for (5), that is, (2) with $t = 0$, become

$$h(x,0) = \begin{cases} H & x < 0, \\ 1 & x > 0, \end{cases}$$

$$u(x,0) = \left(\frac{2}{1+H}\right)^{1/2} \cdot \begin{cases} 1 & x < 0, \\ H & x > 0. \end{cases}, \quad H > 1, \tag{11}$$

or, equivalently, for (7),

$$r(x,0) = \begin{cases} \left(\frac{2}{1+H}\right)^{1/2} - 2\sqrt{H} & x < 0, \\ H\left(\frac{2}{1+H}\right)^{1/2} - 2 & x > 0, \end{cases} \qquad s(x,0) = \begin{cases} \left(\frac{2}{1+H}\right)^{1/2} + 2\sqrt{H} & x < 0, \\ H\left(\frac{2}{1+H}\right)^{1/2} + 2 & x > 0. \end{cases} \tag{12}$$

In what follows, the initial water height jump parameter,

$$\epsilon = 2(\sqrt{H} - 1), \tag{13}$$

plays an important role. It will be shown that it is convenient to utilize the small parameter ϵ rather than $H - 1$ (note that $\epsilon \sim H - 1$ for $0 < H - 1 \ll 1$) so that the far-field conditions for h in Equation (10) are satisfied exactly in the obtained approximate solution. One can see that, if $\epsilon \ll 1$, then $s(x,0)$ in Equation (12) is constant in x to second order in ϵ,

$$s_\pm = 3 + \frac{3}{4}\epsilon + \frac{1}{32}\epsilon^2 + \frac{1}{128}\epsilon^3 \cdot \begin{cases} -3 \\ 1 \end{cases} + \mathcal{O}(\epsilon^4), \tag{14}$$

where $s_\pm = s(h_\pm, u_\pm)$, see (2) and (6). Thus, the initial jump of s across the weak expansion shock solution is of the third order, $s_+ - s_- = -\frac{1}{32}\epsilon^3 + \mathcal{O}(\epsilon^4)$. At the same time, the initial jump in r,

$$r_\pm = -1 + \frac{1}{4}\epsilon \cdot \begin{cases} 3 \\ -5 \end{cases} + \frac{1}{32}\epsilon^2 + \mathcal{O}(\epsilon^3) \tag{15}$$

is of the first order. Thus, for small initial jumps, the RH locus of the expansion shock coincides to $\mathcal{O}(\epsilon^2)$ with the simple (rarefaction) wave locus $s = const$. This observation is similar to the well-known property of systems of hyperbolic conservation laws, in which rarefaction curves (for a given constant state) have third-order contact with shock curves [7]. The difference is that in our calculation, both constant states are varied with H,

keeping the wave speed constant, whereas in the classical case, the wave speed varies along the wave curves, and one of the constant states is fixed.

The purpose of using the small parameter ϵ is due to the fact that $h_\pm = \frac{1}{16}(r_\pm - s_\pm)^2$ exactly satisfies (10), even for the first- and second-order expansions in terms of ϵ in Equation (14) and (15). If one instead expands $s_\pm$, $r_\pm$ in terms of the small parameter $H - 1$, this property will not hold. Although using ϵ or $H - 1$ yields asymptotically equivalent approximate solutions, the sustenance of the far-field behavior in Equation (10) is useful for comparing the asymptotic solution with the numerical solution, as we will do in Section 5.

3. BBM approximation and the structure of the expansion shock

For hyperbolic conservation laws, Riemann initial data such as in Equation (11) provide useful mathematical approximations to physical problems in which the data are actually smooth, as well as being the basis for the method of wave front tracking [8]. For the dispersive problem studied here, the initial transition width turns out to be an important small parameter in the analysis. We therefore introduce

$$0 < \delta \ll 1, \tag{16}$$

as a small scaling parameter characterizing the width (in x) of the transition in the smooth initial data approximating the jump data in Equation (11). The constants in (11) now play the role of far-field data $h_\pm = h(\pm\infty, t)$ and $u_\pm = u(\pm\infty, t)$. The precise structure of the smooth transition will be determined in the course of our analysis. To get some insight into the structure of the evolution of expansion shocks for the Boussinesq system (1), we use the proximity of the system (1) to the BBM equation for the class of Riemann data (11) with small jumps, $0 < \epsilon = 2(\sqrt{H} - 1) \ll 1$. To this end, we convert the full dispersive system (1) to Riemann invariant variables (6), resulting in the system

$$\begin{aligned} r_t + \frac{1}{4}(3r + s)r_x &= \frac{1}{6}(r_{xxt} + s_{xxt}) \\ s_t + \frac{1}{4}(r + 3s)s_x &= \frac{1}{6}(r_{xxt} + s_{xxt}). \end{aligned} \tag{17}$$

A similar change of variables to (6), (8) was previously used in a fully nonlinear model of shallow capillary-gravity waves, the generalized Serre system, to obtain approximate unidirectional models, splitting the slow and fast waves [9]. Here, we demonstrate the utility of these variables for obtaining approximate solutions to the original bidirectional model.

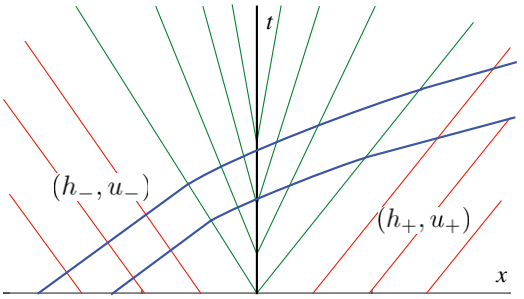

Figure 1. Characteristics in the (x, t)-plane for the expansion shock solution of system (1).

Motivated by the Riemann data expansions (12) and (14) for small jumps, we consider initial data for the Boussinesq system (17) with constant $s = s^{(0)}$. Then, having initially $s = s^{(0)}$ and r exhibiting a jump, we can neglect s_{xxt} in the first equation of (17), at least for $t \ll 1$, and reduce it to the BBM equation

$$v_t + vv_x = \tfrac{1}{6} v_{xxt}\,, \tag{18}$$

provided

$$v = \tfrac{1}{4}(s^{(0)} + 3r). \tag{19}$$

Then, if $v(x, 0) = A\tanh(x/\delta)$, the approximate solution for the expansion shock of the BBM equation (18) is available from [5]. The related behaviors of $h(x, t), u(x, t)$ are then found from (8). The described BBM approximation, while not yet being fully justified asymptotically, provides some useful intuition into the expansion shock structure for the Boussinesq system and in fact, as we see, correctly describes the first-order asymptotic solution.

In Fig. 1, we show schematically the structure of characteristics for the evolution of the Boussinesq stationary expansion shock suggested by the BBM approximation. The smoothed jump initial data for h, u are indicated as subscripts "$-$" for $-x \gg \delta$, and "$+$" for $+x \gg \delta$. In the rarefaction wave, the characteristic speed λ_1 is varying, increasing from left to right, and the characteristics have correspondingly different speeds as they emerge from the shock. Moreover, λ_2 is changing also, so the fast characteristics are curved as they pass through the simple wave. However, the Riemann invariant s is constant on these characteristics, and therefore, takes the value $s_- = s(h_-, u_-)$ to the left, and $s_+ = s(h_+, u_+)$ to the right. As we have shown (see (14)), the jump $s_+ - s_-$ across $x = 0$ is small for small to moderate water height jumps ϵ. As a consequence, s turns out to be roughly

constant across the entire solution except, as we see, in the small, δ-wide region within the expansion shock.

4. Expansion shock for the Boussinesq equations

We now proceed with the detailed asymptotic analysis of expansion shocks for the system (17). Similar to [5], we use matched asymptotic expansions. The key to the analytic construction in [5] is the separable structure of the PDE describing the inner solution with the scaled variables $\xi = x/\delta$, $T = \delta t$. Unfortunately, the Boussinesq equations (17) do not admit such a separation of variables with this scaling of x, t and require a somewhat more sophisticated asymptotic analysis to reveal the detailed internal structure of the expansion shock.

We first consider the inner problem, that is, near the initial smoothed transition. The precise structure of the smoothed Riemann data will be clarified in the analysis below. Our construction will be based on formal expansions in two small parameters: the initial jump in height $\epsilon \sim H - 1$ (Equation (13)) and the jump spatial transition width δ, set by the initial conditions. However, as we see, the resulting solution also provides an excellent approximation for moderate values of $H - 1$.

4.1. Inner solution: first -order approximation

Assuming the spatial scale δ of the inner solution to be set by the smoothed initial data, we seek a solution to Equations (17) in the scaled inner variables $\xi = x/\delta$, $\tau = \mu t$, where the parameter $0 < \mu \ll 1$ is an inverse timescale for the development of an expansion shock, which is to be determined. With these scalings, Equations (17) become

$$\begin{aligned} \mu r^{(\mathrm{in})}_{\tau} + \frac{1}{4\delta}(3r^{(\mathrm{in})} + s^{(\mathrm{in})})r^{(\mathrm{in})}_{\xi} &= \frac{\mu}{6\delta^2}\left(r^{(\mathrm{in})}_{\xi\xi\tau} + s^{(\mathrm{in})}_{\xi\xi\tau}\right) \\ \mu s^{(\mathrm{in})}_{\tau} + \frac{1}{4\delta}(r^{(\mathrm{in})} + 3s^{(\mathrm{in})})s^{(\mathrm{in})}_{\xi} &= \frac{\mu}{6\delta^2}\left(r^{(\mathrm{in})}_{\xi\xi\tau} + s^{(\mathrm{in})}_{\xi\xi\tau}\right). \end{aligned} \tag{20}$$

We wish to find an approximate solution of system (20) that agrees with the initial conditions (12) to some order of accuracy, specifically for $t = \tau = 0$, and $\xi \to \pm\infty$. For this, we assume that the parameter ϵ in (13) is small and expand $r^{(\mathrm{in})}$ and $s^{(\mathrm{in})}$ according to

$$\begin{aligned} r^{(\mathrm{in})}(\xi, \tau) &= r^{(0)} + \epsilon r^{(1)}(\xi, \tau) + \epsilon^2 r^{(2)}(\xi, \tau) + \cdots, \\ s &= s^{(0)} + \epsilon^2 s^{(2)}(\xi, \tau) + \cdots, \end{aligned} \tag{21}$$

where $r^{(0)}$, $r^{(1)}$, $r^{(2)}$, $s^{(0)}$, and $s^{(2)}$ are $\mathcal{O}(1)$ as $\epsilon \to 0$, $\delta \to 0$, $\mu \to 0$. The parameter ϵ is proportional to the initial jump in r from Equation (15), and in the expansion for s we have assumed that $s^{(1)} = 0$, which is consistent with the discussion in the previous section, and could be readily deduced by modifying the analysis below.

Inserting expansions (21) into Equation (20), we obtain

$$\begin{aligned}
&\mu\left(\epsilon r_\tau^{(1)} + \cdots\right) \\
&\quad + \frac{1}{4\delta}\left(3r^{(0)} + s^{(0)} + 3\epsilon r^{(1)} + \epsilon^2(3r^{(2)} + s^{(2)}) + \cdots\right)\left(\epsilon r_\xi^{(1)} + \epsilon^2 r_\xi^{(2)} + \cdots\right) \\
&= \frac{\mu}{6\delta^2}\left(\epsilon r_{\xi\xi\tau}^{(1)} + \epsilon^2\left(r_{\xi\xi\tau}^{(2)} + s_{\xi\xi\tau}^{(2)}\right) + \cdots\right)
\end{aligned} \tag{22}$$

and

$$\begin{aligned}
&\left(\mu\epsilon^2 s_\tau^{(2)} + \cdots\right) + \frac{1}{4\delta}\left(r^{(0)} + 3s^{(0)} + \cdots\right)\left(\epsilon^2 s_\xi^{(2)} + \cdots\right) \\
&= \frac{\mu}{6\delta^2}\left(\epsilon r_{\xi\xi\tau}^{(1)} + \cdots\right).
\end{aligned} \tag{23}$$

Because $\mu \ll 1/\delta$, the leading order term in Equation (22) is

$$\mathcal{O}\left(\frac{\epsilon}{\delta}\right): \quad \frac{1}{4}(3r^{(0)} + s^{(0)})r_\xi^{(1)} = 0, \tag{24}$$

which is solved by

$$r^{(0)} = -\frac{s^{(0)}}{3}. \tag{25}$$

To find an approximate inner solution that balances nonlinearity and dispersion in Equation (22), we require

$$\mu\epsilon \ll \epsilon^2/\delta = \mathcal{O}(\mu\epsilon/\delta^2). \tag{26}$$

This determines the inverse timescale μ in terms of the transition width δ and jump amplitude parameter ϵ. We take

$$\mu = \delta\epsilon. \tag{27}$$

Proceeding under these assumptions, we obtain from Equation (22)

$$\mathcal{O}\left(\frac{\epsilon^2}{\delta}\right): \quad r^{(1)}r_\xi^{(1)} = \frac{2}{9}r_{\xi\xi\tau}^{(1)}. \tag{28}$$

We can now solve this equation by separation of variables

$$r^{(1)}(\xi, \tau) = a(\tau)f(\xi), \tag{29}$$

where

$$\frac{2\dot{a}}{9a^2} = \frac{ff'}{f''} = -K, \tag{30}$$

and $K > 0$ is the separation constant. We determine a and f as for BBM in [5]

$$a(\tau) = \frac{A}{\frac{9}{2}AK\tau + 1}, \quad f(\xi) = B\tanh\left(\frac{B}{2K}\xi\right), \tag{31}$$

where $A > 0$ and $B > 0$ are parameters to be determined. We choose the parameters

$$B = 1, \quad K = \frac{1}{2}, \tag{32}$$

and retain the amplitude parameter A, which will be determined by the RH locus, so that the solution (31) is

$$a(\tau) = \frac{A}{\frac{9}{4}A\tau + 1}, \quad f(\xi) = \tanh(\xi). \tag{33}$$

Then, the approximate inner expansion shock solution to first order in ϵ can be written

$$r^{(\mathrm{in})}(\xi, \tau) = -\frac{s^{(0)}}{3} + \frac{\epsilon A}{\frac{9}{4}A\tau + 1}\tanh(\xi) + \mathcal{O}(\epsilon^2), \tag{34}$$

$$s^{(\mathrm{in})}(\xi, \tau) = s^{(0)} + \mathcal{O}(\epsilon^2). \tag{35}$$

To determine the free parameters $s^{(0)}$ and A in terms of the initial data, we evaluate the solution (34), (35) at $t = 0$, $\xi \to \pm\infty$, and compare it with the first-order small-jump expansions of the initial conditions (12) incorporating the RH locus:

$$r_\pm = -\frac{s^{(0)}}{3} \pm \epsilon A + \mathcal{O}(\epsilon^2), \tag{36}$$

$$s_\pm = s^{(0)} + \mathcal{O}(\epsilon^2), \quad \xi \to \pm\infty. \tag{37}$$

Comparing Equations (36) and (37) with Equations (14) and (15), we find

$$s^{(0)} = 3 + \frac{3}{4}\epsilon, \quad A = 1. \tag{38}$$

We note that the constructed first-order inner solution (34), (35), (38) for the expansion shock simultaneously incorporates the simple wave locus $s_- = s_+ = s^{(0)}$ of the shallow-water equations (7) *and* the RH condition $v_- + v_+ = 0$ for the stationary shock of the simple wave equation

$v_t + vv_x = 0$, where $v = \frac{1}{4}(s^{(0)} + 3r)$ (recall Equation (19)). This is nothing but the dispersionless limit of the BBM equation (18). Indeed, one can see that the first-order solution written in terms of v agrees with the inner solution for the BBM expansion shock obtained in [5].

4.2. Inner solution: second-order approximation

To obtain the $\mathcal{O}(\epsilon^2)$ correction, we consider Equation (23), from which we deduce, using $r^{(1)} = a(\tau)f(\xi)$ from the previous subsection,

$$\mathcal{O}\left(\frac{\epsilon^2}{\delta}\right): \quad s^{(2)}_{\xi} = \frac{1}{12} r^{(1)}_{\xi\xi\tau} = \frac{1}{12}\dot{a}(\tau) f''(\xi). \tag{39}$$

This equation is solved with

$$s^{(2)}(\xi, \tau) = \frac{1}{12}\dot{a}(\tau) f'(\xi) + C = -\frac{3\,\mathrm{sech}^2(\xi)}{16\left(1 + \frac{9}{4}\tau\right)^2} + C. \tag{40}$$

The constant of integration C could at this stage be a function of τ, but it will be determined below by matching to the far field, so it is necessarily constant.

We now proceed to the next order equation in (22), assuming that $\delta\epsilon^2 \ll \epsilon^3/\delta$, implying the basic small parameter ordering

$$\delta \ll \epsilon^{1/2}. \tag{41}$$

We find the equation for $r^{(2)}$:

$$\mathcal{O}\left(\frac{\epsilon^3}{\delta}\right): \quad r^{(2)}_{\xi\xi\tau} - \frac{9}{2}(r^{(1)} r^{(2)})_{\xi} = \frac{3}{2} s^{(2)} r^{(1)}_{\xi} - s^{(2)}_{\xi\xi\tau}. \tag{42}$$

We observe that this equation has solutions of the form

$$r^{(2)}(\xi, \tau) = a^2(\tau) g(\xi) - \frac{C}{3}, \tag{43}$$

in which $a(\tau)$ is given in (33). Then g satisfies

$$g'' + (fg)' = \frac{1}{16}(f'^2 + 3f''') = \frac{1}{16}(f' - f' f^2 + 3f'''). \tag{44}$$

Integrating, we obtain

$$g' + fg = \frac{1}{16}\left(f - \frac{1}{3}f^3 + 3f'' + \frac{1}{3}D\right), \tag{45}$$

where D is a constant of integration. An integrating factor for this equation is $\cosh(\xi)$. We therefore obtain

$$g(\xi) = \frac{1}{16}\left(\frac{2}{3} + \frac{17}{3}\,\mathrm{sech}^2(\xi) + \frac{1}{3}D\tanh(\xi) + \frac{1}{3}E\,\mathrm{sech}(\xi)\right), \tag{46}$$

where E is an additional constant of integration. Then the approximate inner solution for the expansion shock to second order in ϵ becomes

$$\begin{aligned} r^{(\mathrm{in})}(\xi,\tau) \;&\sim -1+\epsilon\left(-\frac{1}{4}+\frac{\tanh(\xi)}{1+\frac{9}{4}\tau}\right)\\ &\quad+\frac{\epsilon^2}{3}\left(-C+\frac{2+17\,\mathrm{sech}^2(\xi)+D\tanh(\xi)+E\,\mathrm{sech}(\xi)}{16\left(1+\frac{9}{4}\tau\right)^2}\right),\\ s^{(\mathrm{in})}(\xi,\tau) \;&\sim 3+\frac{3}{4}\epsilon+\epsilon^2\left(C-\frac{3\,\mathrm{sech}^2(\xi)}{16\left(1+\frac{9}{4}\tau\right)^2}\right). \end{aligned} \tag{47}$$

The constant E is a free parameter, not determined at this order. We therefore set $E=0$, without loss of generality, by appropriate choice of initial conditions. To determine the remaining parameters C and D, we invoke the smoothed Riemann data (12) and evaluate the approximate solution (47) at $t=0$ for $r^{(\mathrm{in})}$ and $s^{(\mathrm{in})}$ as $\xi\to\pm\infty$, yielding (cf. (36) and (37)),

$$\begin{aligned} r_\pm &= -1+\epsilon\left(-\frac{1}{4}\pm 1\right)+\epsilon^2\left(-\frac{C}{3}+\frac{1}{24}\pm\frac{D}{48}\right)+\mathcal{O}(\epsilon^3),\\ s_\pm &= 3+\frac{3}{4}\epsilon+C\epsilon^2+\mathcal{O}(\epsilon^3), \end{aligned} \tag{48}$$

which satisfy the RH locus expansions (14) and (15) to $\mathcal{O}(\epsilon^2)$ if we take

$$C=\frac{1}{32},\quad D=0, \tag{49}$$

which, together with (47), fully defines the second-order inner solution, beyond the BBM approximation as

$$\begin{aligned} r^{(\mathrm{in})}(\xi,\tau) &\sim -1+\epsilon\left(-\frac{1}{4}+\frac{\tanh(\xi)}{1+\frac{9}{4}\tau}\right)+\frac{\epsilon^2}{48}\left(-\frac{1}{2}+\frac{2+17\,\mathrm{sech}^2(\xi)}{\left(1+\frac{9}{4}\tau\right)^2}\right),\\ s^{(\mathrm{in})}(\xi,\tau) &\sim 3+\frac{3}{4}\epsilon+\frac{\epsilon^2}{16}\left(\frac{1}{2}-\frac{3\,\mathrm{sech}^2(\xi)}{\left(1+\frac{9}{4}\tau\right)^2}\right). \end{aligned} \tag{50}$$

4.3. Outer solution

For matching purposes, it is natural to set the timescale for the outer scaling to be the same as the timescale of the inner scaling $\tau=\mu t=\delta\epsilon t$, using (27). Along with that, we use the long wave, hydrodynamic scaling $X=\delta x$, which is independent of the jump amplitude parameter ϵ. Then the leading order (in δ) equations from (17) are the dispersionless shallow-water

equations

$$\begin{aligned}\epsilon r_\tau^{(\mathrm{out})} + \frac{1}{4}(3r^{(\mathrm{out})} + s^{(\mathrm{out})})r_X^{(\mathrm{out})} = 0,\\ \epsilon s_\tau^{(\mathrm{out})} + \frac{1}{4}(r^{(\mathrm{out})} + 3s^{(\mathrm{out})})s_X^{(\mathrm{out})} = 0.\end{aligned} \tag{51}$$

We expect a simple wave solution, which we expand as

$$\begin{aligned}s^{(\mathrm{out})}(X,\tau) &= 3 + \frac{3}{4}\epsilon + \frac{1}{32}\epsilon^2 + \cdots,\\ r^{(\mathrm{out})}(X,\tau) &= -1 + \epsilon\left(-\frac{1}{4} + r_1(X,\tau)\right) + \epsilon^2\left(-\frac{1}{96} + r_2(X,\tau)\right) + \cdots.\end{aligned} \tag{52}$$

With these expansions, the Equation (51) for $s^{(\mathrm{out})}$ is identically satisfied. The equation for $r^{(\mathrm{out})}$, expanded in powers of ϵ, yields to leading order

$$\mathcal{O}(\epsilon^2): \quad r_{1,\tau} + \frac{3}{4}r_1 r_{1,X} = 0, \tag{53}$$

which can be solved with

$$r_1(X,\tau) = F_1^{(\operatorname{sgn} X)}\left(\tau - \frac{4X}{3r_1}\right), \tag{54}$$

where we use the functions $F_1^{(\pm)}$ depending on whether $\pm X > 0$. Matching this to the inner solution (50) at $\mathcal{O}(\epsilon)$ yields

$$\lim_{X\to 0^\pm} r_1(X,\tau) = F_1^{(\pm)}(\tau) = \lim_{\xi\to\pm\infty} r^{(1)}(\xi,\tau) = \pm\frac{1}{1+\frac{9}{4}\tau}. \tag{55}$$

Then,

$$r_1 = \frac{\operatorname{sgn} X}{1 + \frac{9}{4}\tau - \frac{3X}{r_1}}, \tag{56}$$

which is solved by

$$r_1(X,\tau) = \frac{\operatorname{sgn} X + 3X}{1+\frac{9}{4}\tau}. \tag{57}$$

Proceeding to the next order in the expansion of Equation (51) yields an equation for r_2

$$\mathcal{O}(\epsilon^3): \quad r_{2,\tau} + \frac{3}{4}(r_1 r_2)_X = 0. \tag{58}$$

One can verify by direct substitution that

$$r_2(X,\tau) = F_2^{(\operatorname{sgn} X)}\frac{1+3|X|}{\left(1+\frac{9}{4}\tau\right)^2}, \tag{59}$$

solves Equation (58). Matching to the inner solution (50), we obtain

$$\lim_{X\to 0^{\pm}} r_2(X,\tau) = F_2^{\pm}\frac{1}{\left(1+\frac{9}{4}\tau\right)^2} = \lim_{\xi\to\pm\infty} r^{(2)}(\xi,\tau) = \frac{1}{24\left(1+\frac{9}{4}\tau\right)^2}, \tag{60}$$

so that $F_2^+ = F_2^- = 1/24$, yielding the second-order correction to the outer solution

$$r_2(X,\tau) = \frac{1+3|X|}{24\left(1+\frac{9}{4}\tau\right)^2}. \tag{61}$$

The approximate outer solution therefore has the form

$$\begin{aligned} r^{(\mathrm{out})}(X,\tau) &= -1+\epsilon\left(-\frac{1}{4}+\frac{\operatorname{sgn} X+3X}{1+\frac{9}{4}\tau}\right) \\ &\quad +\frac{\epsilon^2}{24}\left(-\frac{1}{4}+\frac{1+3|X|}{\left(1+\frac{9}{4}\tau\right)^2}\right)+\mathcal{O}(\epsilon^3), \\ s^{(\mathrm{out})}(X,\tau) &= 3+\frac{3}{4}\epsilon+\frac{1}{32}\epsilon^2+\mathcal{O}(\epsilon^3). \end{aligned} \tag{62}$$

Note that for the dispersionless Equation (51) to be a valid asymptotic approximation of the full Boussinesq eqs. (17) to $\mathcal{O}(\epsilon^3)$, we require the dispersive term to be negligible to the order considered, that is, $\epsilon\delta^3 \ll \epsilon^3$ or $\delta \ll \epsilon^{2/3}$. This is a less stringent condition on scale separation than the restriction (41) applied for the calculation of the inner solution.

This approximate outer solution is only valid within an expanding region. We invoke continuous matching to the far-field along the two characteristic lines

$$X = c_{\pm}\tau, \tag{63}$$

where $c_{\pm}$ is determined by the requirement

$$r^{(\mathrm{out})}(c_{\pm}\tau,\tau) = r_{\pm}. \tag{64}$$

A calculation using (15), (62) yields the speeds

$$c_{\pm} = \pm\frac{3}{4}+\frac{1}{32}\epsilon+\cdots. \tag{65}$$

Matching to the far field, we obtain the approximate, piecewise smooth outer solution

$$r^{(\mathrm{out})}(X,\tau) = -1+\epsilon\begin{cases} -\frac{5}{4}+\frac{1}{32}\epsilon & \frac{X}{\tau}\le c_-,\\ -\frac{1}{4}+\frac{\operatorname{sgn}X+3X}{1+\frac{9}{4}\tau}+\frac{\epsilon}{24}\left(-\frac{1}{4}+\frac{1+3|X|}{\left(1+\frac{9}{4}\tau\right)^2}\right) & c_-<\frac{X}{\tau}<c_+,\\ \frac{3}{4}+\frac{1}{32}\epsilon & c_+\le\frac{X}{\tau}, \end{cases} +\mathcal{O}(\epsilon^3), \tag{66}$$

$$s^{(\mathrm{out})}(X,\tau) = 3+\frac{3}{4}\epsilon+\frac{1}{32}\epsilon^2+\mathcal{O}(\epsilon^3).$$

4.4. Uniformly valid asymptotic solution

To construct a uniformly valid (in x) asymptotic solution to $\mathcal{O}(\epsilon^2)$ in r and s, we introduce the composite solution

$$\begin{aligned} r(x,t) &= r^{(\mathrm{in})}(x/\delta,\delta\epsilon t)+r^{(\mathrm{out})}(\delta x,\delta\epsilon t)-r^{(\mathrm{overlap})}(x,t;\delta,\epsilon),\\ s(x,t) &= s^{(\mathrm{in})}(x/\delta,\delta\epsilon t)+s^{(\mathrm{out})}(\delta x,\delta\epsilon t)-s^{(\mathrm{overlap})}(x,t;\delta,\epsilon). \end{aligned} \tag{67}$$

We subtract the "overlap" portion (common to both the inner and outer solutions) so that we do not double count the matching region. We therefore have

$$\begin{aligned} r^{(\mathrm{overlap})}(x,t;\delta,\epsilon) &\sim -1+\epsilon\left(-\frac{1}{4}+\frac{\operatorname{sgn}X}{1+\frac{9}{4}\tau}\right)+\frac{\epsilon^2}{24}\left(-\frac{1}{4}+\frac{1}{\left(1+\frac{9}{4}\tau\right)^2}\right),\\ s^{(\mathrm{overlap})}(x,t;\delta,\epsilon) &\sim 3+\frac{3}{4}\epsilon+\frac{1}{32}\epsilon^2. \end{aligned} \tag{68}$$

Then the uniformly valid, composite asymptotic solution for an expansion shock is

$$\begin{aligned} r(x,t;\delta,\epsilon) &\sim -1+\epsilon\left(\frac{\tanh\left(\frac{x}{\delta}\right)-\operatorname{sgn}(x)}{1+\frac{9}{4}\delta\epsilon t}+G_1(x,t;\delta,\epsilon)\right)\\ &\quad+\epsilon^2\left(\frac{17\operatorname{sech}^2\left(\frac{x}{\delta}\right)}{48\left(1+\frac{9}{4}\delta\epsilon t\right)^2}+G_2(x,t;\delta,\epsilon)\right),\\ s(x,t) &\sim 3+\frac{3}{4}\epsilon+\frac{\epsilon^2}{16}\left(\frac{1}{2}-\frac{3\operatorname{sech}^2\left(\frac{x}{\delta}\right)}{\left(1+\frac{9}{4}\delta\epsilon t\right)^2}\right), \end{aligned} \tag{69}$$

$$G_1(x,t;\delta,\epsilon) = \begin{cases} -\frac{5}{4} & \frac{x}{\epsilon t}\le c_-,\\ -\frac{1}{4}+\frac{\operatorname{sgn}(x)+3\delta x}{1+\frac{9}{4}\delta\epsilon t} & c_-<\frac{x}{\epsilon t}<c_+,\\ \frac{3}{4} & c_+\le\frac{x}{\epsilon t}, \end{cases}$$

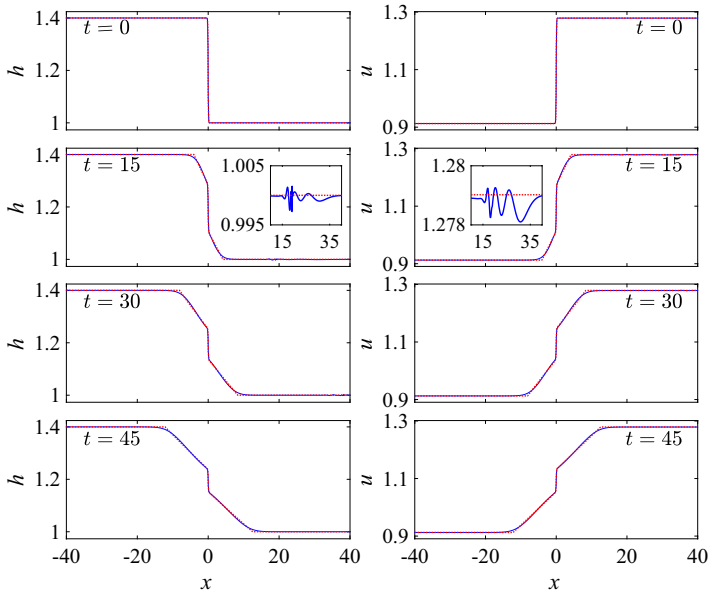

Figure 2. Numerical simulation of the Boussinesq equation for expansion shock initial data in physical variables h, u (solid) compared with the the uniform asymptotic approximation (dotted) for $H = 1.4$, $\epsilon \approx 0.366$, $\delta = 0.1$. The insets correspond to a zoomed in region when $t = 15$ that depicts the $\mathcal{O}(\epsilon^3)$ radiation generated by inaccuracy in the initial condition.

$$G_2(x,t;\delta,\epsilon) = \begin{cases} \dfrac{1}{32} & \dfrac{x}{\epsilon t} \le c_-, \\ -\dfrac{1}{96} + \dfrac{1+3\delta|x|}{24\left(1+\frac{9}{4}\delta\epsilon t\right)^2} & c_- < \dfrac{x}{\epsilon t} < c_+, \\ \dfrac{1}{32} & c_+ \le \dfrac{x}{\epsilon t}, \end{cases}$$

where $c_\pm$ is given in (65). This solution can be used in (6) to reconstruct the expansion shock water height h and horizontal velocity u.

5. Numerical simulation

We validate the asymptotic analysis of Section 4.4 with direct numerical simulations of the Boussinesq equations (1) with initial data consisting of the approximate expansion shock solution (69) evaluated at $t = 0$. The numerical method is described in the Appendix.

Figure 2 depicts the numerical evolution of h and u with an initial jump in h from unity to $H = 1.4$ and the transition width $\delta = 0.1$. The boundary

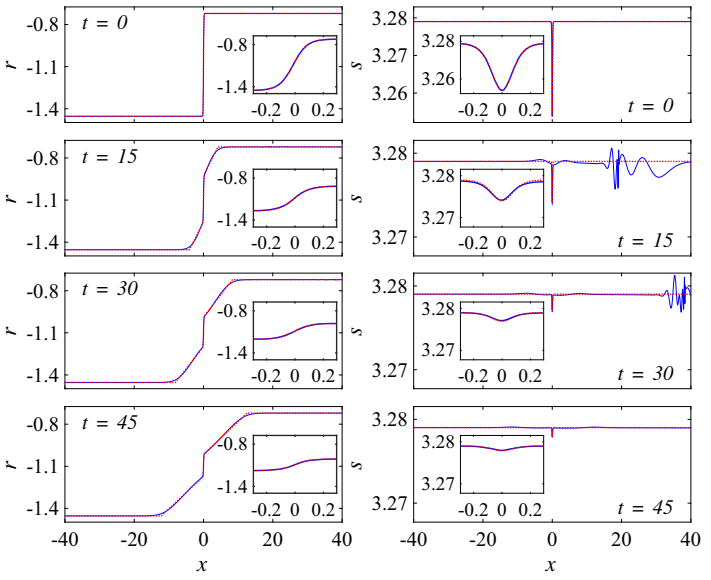

Figure 3. Numerical simulation of the Boussinesq equation for expansion shock initial data in the transformed variables r, s (solid) compared with the uniform asymptotic approximation (dotted) for $H = 1.4$, $\epsilon \approx 0.366$, $\delta = 0.1$. The insets reveal the zoomed in expansion shock structure. Note the change in the s amplitude scale for $t > 0$.

conditions $u_{\pm}$, determined by eqs. (8), (14), and (15), satisfy the RH locus (4) to order ϵ^2. The sharp initial step evolves into an expansion shock that algebraically decays between noncentered rarefaction waves propagating left and right. The uniform asymptotic approximation (69) closely follows the numerical solution; the most noticeable deviations occurring at the weak discontinuities, where the rarefactions meet the far-field boundary conditions with a jump in the first derivative of the asymptotic solution. A close examination reveals the generation of a small amplitude dispersive wavepacket that propagates to the right (see insets at $t = 15$). This is due to the fact that the initial data only approximately corresponds to an expansion shock, accurate to order ϵ^2. For this simulation, $\epsilon = 2(\sqrt{H} - 1) \approx 0.366$, for which $\epsilon^{5/2} \approx 0.0813$, larger than the size of the dispersive wavepacket.

It is revealing to examine the evolution of the scaled Riemann variables r and s in Fig. 3. The variable r evolves much like h and u, with order one changes in amplitude. The smooth, decaying expansion shock structure is accurately resolved by the asymptotic approximation, as shown in the insets. The evolution of s, on the other hand, is at a much smaller amplitude scale. Recall that the RH locus (4) leads to an order ϵ^3 jump in s across an expansion shock. This variation in s is not captured by our asymptotic approximation (69) and is the source of the dispersive

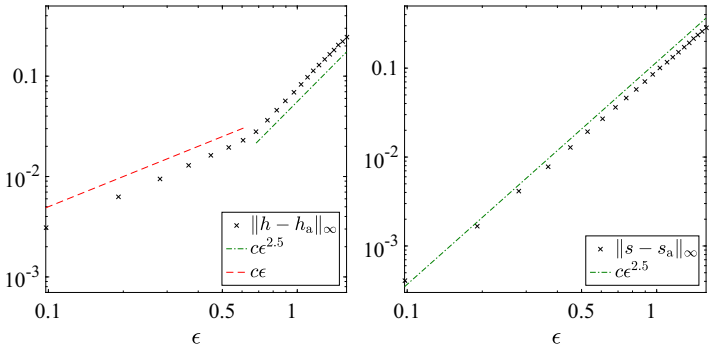

Figure 4. Error analysis of approximate expansion shock solution for variable ϵ and fixed $\delta = 0.1$. We compare simulations of the Boussinesq equations with the asymptotic solution (69) in the infinity norm for h (left) and s (right).

wavepacket that propagates away from the initial transition. Note that although the oscillations appear sharp in the figure, they are smoothly and accurately resolved by the numerical simulation. Presumably, a higher order correction to the obtained expansion shock approximation (69) would reduce the amplitude of this wavepacket. Nevertheless, the initial, order ϵ^2 amplitude dip in s at the transition is apparent and accurately captured by the asymptotic approximation.

We undertake an error analysis of the asymptotic expansion shock solution (69) by performing numerical simulations with variable initial jump height parameter ϵ and fixed transition width $\delta = 0.1$. Figure 4 shows a summary of the results, comparing the infinity norm difference between the asymptotic approximation, denoted by the subscript "a," and the numerical solution for both h and s as ϵ is varied. The errors in u and r are similar to those for h. The norm difference is computed across the entire simulation domain, that is, for $x \in [-L, L]$ and $t \in [0, T]$. For these simulations $L = 120$, $T = 45$. Both h and s show an approximately $\mathcal{O}(\epsilon^{5/2})$ dependence of the error over a portion or all of the jump heights considered. The dominant contribution to these errors is due to the dispersive wavepacket that is generated by the discrepancy in the approximate initial data (recall the insets in Fig. 2). The error is consistent with the formal second-order accuracy of the asymptotic solution. It is striking that the asymptotic solution exhibits small error, even for values of ϵ above one. Below $\epsilon = 0.6$, the error in h decays at a slower rate approximately proportional to ϵ. This is because the dominant error contribution now comes from the region where the noncentered rarefaction waves are matched to the constant background, Equation (64). The higher order approximation fails to resolve this region, which is smoothed in the numerical solution by dispersion. This discrepancy is visible in Fig. 2.

6. Discussion

Decaying expansion shocks were recently identified as robust solutions to conservation laws of nonevolutionary type that naturally arise in shallow-water theory. In [5], we studied these shocks in the framework of the unidirectional BBM equation, using matched asymptotic expansions. In the present paper, the analysis of [5] is extended to a bidirectional regularized Boussinesq system [1]. The extension to the bidirectional case is more complicated, and has revealed further structure of expansion shocks exhibiting subtle but essential features that appear in the second-order corrections of the matched asymptotic expansion, while the first-order solution is equivalent to the BBM expansion shock. The key approach to our analysis of Boussinesq expansion shocks is the use of Riemann invariants of the underlying ideal shallow-water equations as field variables in the full dispersive system. Another important aspect is the requirement of the balance between two small parameters: the width δ of the smoothed Riemann data satisfying the stationary expansion shock RH conditions and the value of the initial jump of the water height, measured by ϵ. The product $\mu = \epsilon\delta$ then sets the inverse timescale for the algebraic decay of the expansion shock.

The expansion shock phenomenon was shown in [5] to be highly robust. In [5], finite perturbations to the expansion shock for BBM were considered numerically and it was found that an overall shift of the background state yields a mismatch in the far field data that is resolved by the generation of solitary waves, the number depending upon the asymmetry of the data, while the expansion shock structure is fully retained. Because the BBM equation is a unidirectional asymptotic reduction of the regularized Boussinesq system, it is expected that a similar solitary wave shedding will occur in the Boussinesq case as well. Therefore, a natural extension of this work is the consideration of jump initial data (2) that does not lie on the RH locus (4). The bidirectional nature of the Boussinesq equations (1) suggests a richer set of outcomes.

The comparison of the obtained second order asymptotic formula with accurate numerical solution of the smoothed Riemann problem for the Boussinesq system reveals remarkable agreement, even for relatively large initial jumps, beyond the formal applicability of our asymptotic analysis. In conclusion, we note that, in considering more general initial data, the use of "dispersionless" Riemann invariants as dependent variables in the full system may give insight into the structure of solutions, because the interaction between the two fields occurs primarily through the dispersive terms, except where waves collide.

Acknowledgments

The research of MS and MH is supported by National Science Foundation grants DMS-1517291 and CAREER DMS-1255422, respectively.

Appendix

A pseudospectral Fourier spatial discretization with standard fourth-order Runge–Kutta timestepping is utilized. We discretize the domain $[-L, L]$ according to $x_n = -L + 2Ln/N$, $n = 0, \cdots, N-1$. To accommodate non-periodic boundary conditions in h and u, the spatial derivatives $g = h_x$, $v = u_x$ are numerically evolved according to

$$\begin{aligned} g_t + (ug)_x + (hv)_x &= 0, \\ v_t + (uv)_x + g_x - \frac{1}{3} v_{xxt} &= 0. \end{aligned} \tag{A1}$$

By choosing a sufficiently large domain L, the boundary quantities $|h(\pm L, t) - h_\pm|$ and $|u(\pm L, t) - u_\pm|$ are maintained to within 10^{-9} for the duration of the simulation, therefore g and v can be treated as localized, periodic functions. Each undifferentiated term in Equation (A1) is spatially localized, therefore we can compute their derivatives in spectral space, for example,

$$\mathcal{F}\{(ug)_x\}_n = ik_n \mathcal{F}\{ug\}_n, \quad n = -N/2, \cdots, N/2 - 1, \tag{A2}$$

where $\mathcal{F}$ is the discrete, finite Fourier series operator, efficiently implemented via the fast Fourier transform, and $k_n = n\pi/L$ are the discrete wavenumbers. The function h is approximated by an accumulation of its derivative g according to

$$h(x_n, t) = h_- + \mathcal{F}^{-1}\{\tilde{g}(t)\}_n + \frac{1}{2L}(h_+ - h_-)(x_n + L), \tag{A3}$$

where

$$\tilde{g}_n(t) = \begin{cases} -\dfrac{2L}{N} \displaystyle\sum_{m=-N/2}^{N/2-1} x_m g(x_m, t) & n = 0 \\ \dfrac{\hat{g}_n(t)}{ik_n} & n \neq 0 \end{cases}. \tag{A4}$$

The sum for $n = 0$ in (A4) is a trapezoidal approximation of the integral $\int_{-L}^{L} x g(x, t) dx$ so that an accurate, efficient reconstruction of h from g is achieved. A similar computation is performed to obtain u.

Time evolution is performed on the spectral, Fourier coefficients using the standard fourth-order Runge–Kutta method. The nonlocal character of the dispersive term $v_{xxt}/3$ in Equation (A1) is not stiff so we use a timestep of 0.002 and evolve to $t = 45$. The domain size is $L = 120$ (Figs. 2 and 3 show only a portion of the domain) and the Fourier truncation is $N = 2^{14}$. The accuracy of the numerical computation is monitored by ensuring that the conserved quantities $|\int_{-L}^{L} g(x,t)dx - h_+ + h_-|$ and $|\int_{-L}^{L} v(x,t)dx - u_+ + u_-|$ are maintained to less than 10^{-14} and the Fourier components $|\mathcal{F}\{g\}_n|$, $|\mathcal{F}\{v\}_n|$, $n = -N/2, \ldots, N/2-1$ decay to about 10^{-8}, within the expected value given boundary deviations of about 10^{-9}.

References

1. G. B. Whitham, *Linear and Nonlinear Waves*, Wiley, New York, 1974.
2. J. L. Bona, M. Chen, and J. C. Saut, Boussinesq equations and other systems for small–amplitude long waves in nonlinear dispersive media. I: Derivation and linear theory, *J. Nonlinear Sci.* 12:283–318 (2002).
3. G. A. El and M. A. Hoefer, Dispersive shock waves and modulation theory, *Physica D* 33:11–65 (2016).
4. G. A. El, M. A. Hoefer and M. Shearer, Dispersive and diffusive-dispersive shock waves for nonconvex conservation laws, *SIAM Rev.* 59:3–61 (2017).
5. G. A. El, M. A. Hoefer, and M. Shearer, Expansion shock waves in regularized shallow water theory, *Proc. Roy. Soc. Lond.* 472:20160141 (2016).
6. P. Sprenger and M. A. Hoefer, Shock waves in dispersive hydrodynamics with nonconvex dispersion, *SIAM J. Appl. Math.* 77:26–50 (2017).
7. P. D. Lax, Hyperbolic systems of conservation Laws II, *Comm. Pure Appl. Math.* 10:537–566 (1957).
8. A. Bressan, *Hyperbolic Systems of Conservation Laws: The One-Dimensional Cauchy Problem*, Oxford Univ. Press, New York, 2000.
9. F. Dias and P. Milewski, On the fully-nonlinear shallow-water generalized Serre equations, *Phys. Lett. A*, 374:1049–1053 (2010).

Loughborough University Loughborough
University of Colorado
North Carolina State University

(Received November 3, 2016)